NANO LETTERS

2008
Vol. 8, No. 8
2551-2555

Synthesis and Photovoltaic Application of Copper(I) Sulfide Nanocrystals

Yue Wu,[†,‡] Cyrus Wadia,[†,‡,§] Wanli Ma,[‡] Bryce Sadtler,[‡] and A. Paul Alivisatos*[,‡,||,⊥]

Department of Chemistry, Energy and Resources Group, and Department of Materials Science and Engineering, University of California, Berkeley, California 94720, and Materials Science Division, Lawrence Berkeley National Laboratory, Berkeley, California 94720

Received June 24, 2008; Revised Manuscript Received July 2, 2008

ABSTRACT

We present the rational synthesis of colloidal copper(I) sulfide nanocrystals and demonstrate their application as an active light absorbing component in combination with CdS nanorods to make a solution-processed solar cell with 1.6% power conversion efficiency on both conventional glass substrates and flexible plastic substrates with stability over a 4 month testing period.

Semiconductor nanostructures are promising building blocks for future-generation photovoltaic devices, such as dye-sensitized solar cells,[1–3] all-inorganic nanoparticle solar cells,[4–6] and hybrid nanocrystal−polymer composite solar cells.[7–10] All of these could offer processing, scale, and cost advantages when compared with conventional single crystal and thin film solar cells. One of the most challenging aspects in this area is to find a semiconductor material with a suitable band gap, near 1 eV for a conventional, single-gap device, which can be made in nanostructured form, using earth-abundant elements, and of environmentally benign composition. Here, we explore a candidate material satisfying these requirements: copper(I) sulfide, Cu_2S. Cu_2S is an indirect gap semiconductor with a bulk bandgap of 1.21 eV.[11] Its use in combination with CdS as a solar cell material was extensively investigated between the 1960s and 1980s.[12–17] In thin film studies, Cu_2S/CdS solar cells did show significant promise, but copper diffusion into and doping of the CdS layer led to long-term performance degradation and ultimately abandonment of this system. With the advent of nanocrystal-based approaches which can use much milder processing conditions, and in which diffusion and doping issues take on entirely new character, it is well worthwhile to re-examine this material combination. CdS nanocrystals are of course widely available and can be synthesized with exquisite control over size, shape, and new processing approaches.[18–20] In contrast, there are only a few reports of Cu_2S nanocrystal synthesis.[21–23]

Our synthesis of colloidal Cu_2S nanocrystals involves an injection reaction between copper(II) acetylacetonate and ammonium diethyldithiocarbamate in a mixed solvent of dodecanethiol and oleic acid.[24] X-ray diffraction (XRD) studies (Figure 1a) show the materials prepared in this way are hexagonal chalcocite Cu_2S (JCPDS 026−1116, Figure 1a, red lines). Low-resolution transmission electron microscopy (TEM) studies (Figure 1b) show nanocrystals with an average size of 5.4 ± 0.4 nm. High-resolution TEM studies (upper inset, Figure 1b) confirm that the observed nanocrystals are Cu_2S and show several important features. First, the TEM data demonstrate clearly that the Cu_2S nanocrystals are single crystal structures. Second, these Cu_2S nanocrystals have a well-defined hexagonal-faceted structure (dashed line, upper inset, Figure 1b). Third, the reciprocal lattice peaks, which were obtained from two-dimensional Fourier transforms (2DFT) of the lattice-resolved image (low inset, Figure 1b) can be indexed to the hexagonal structure of Cu_2S with the zone axes along the $[1\bar{2}\ 1\ \bar{3}]$ direction.

The optical properties of the Cu_2S nanocrystals have been studied by UV−visible (UV−vis) absorption spectroscopy and photoluminescence (PL) to further assess their quality. A representative UV−vis spectrum[25] (Figure 1c) of the Cu_2S nanocrystals shows a wide absorption up to approximately 1000 nm. Lastly, PL studies[25] (inset, Figure 1c) show a single peak centered at 1.32 eV, which is similar with reported bulk value of 1.21 eV,[11] with a full-width at half-maximum (fwhm) of 0.17 eV.

* Corresponding author. E-mail: alivis@berkeley.edu
† These authors contributed equally to this work.
‡ Department of Chemistry, University of California.
§ Energy and Resources Group, University of California.
|| Department of Materials Science and Engineering, University of California.
⊥ Lawrence Berkeley National Laboratory.

10.1021/nl801817d CCC: $40.75
Published on Web 07/24/2008

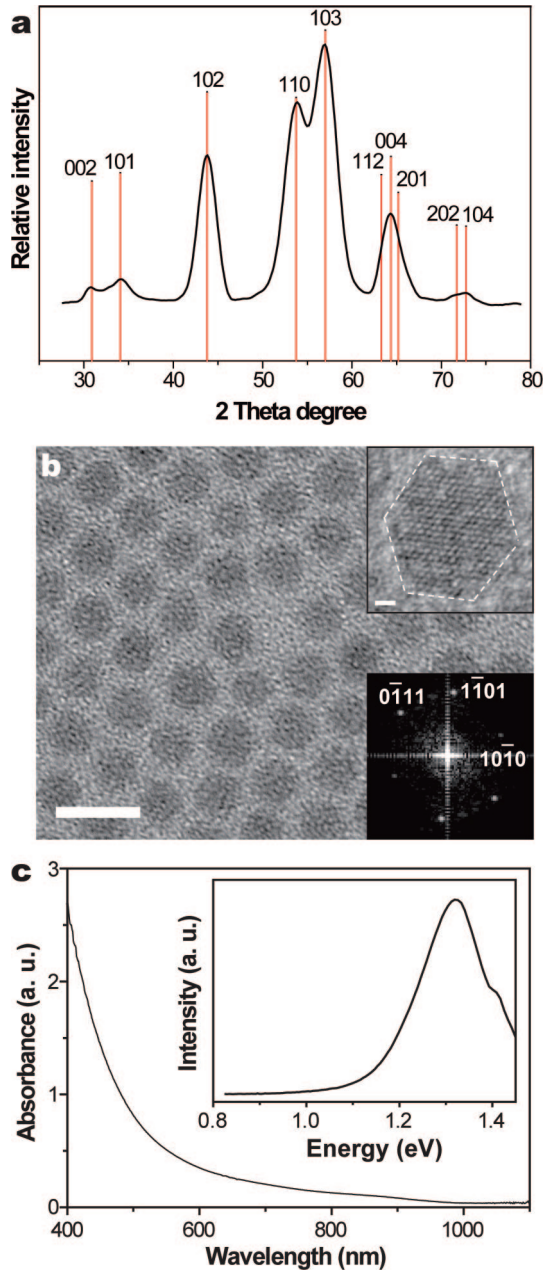

Figure 1. Structural characterization of Cu_2S nanocrystals. (a) XRD diffraction pattern of Cu_2S nanocrystals, which can be indexed to hexagonal Cu_2S (JCPDS 026−1116, red lines). (b) TEM image of Cu_2S nanocrystals with an average diameter of ca. 5.4 nm. The scale bar is 10 nm. Upper inset, high magnification TEM image of Cu_2S nanocrystal shows single crystal hexagonal faceted structure. The scale bar is 1 nm. Lower inset, 2DFT of the image showing the $[1\bar{2}1\bar{3}]$ zone axis of Cu_2S. (c) UV−vis. absorption spectrum of Cu_2S nanocrystals shows a wide absorption up to ca. 1000 nm. Inset, PL spectrum shows a single peak centered at 1.32 eV.

The single crystal Cu_2S nanocrystals have potential photovoltaic application, and we have explored this possibility. We prepared solar cell devices through a low temperature ($\leq$150 °C) solution process[26] in which the critical heterojunction is formed between a layer of spin-cast Cu_2S nanocrystals and a layer of spin-cast CdS nanorods (Figure 2a). The thickness of the Cu_2S nanocrystal layer and the CdS nanorod layer are measured to be around 300 and 100 nm, respectively, with total film surface roughness to be less than 4 nm (inset, Figure 2b) and an average optical density of 1.1.

Representative current density (J)−voltage (V) characteristics recorded on the as-made photovoltaic device show typical rectification behavior under zero illumination (black curve, Figure 3a). Under a standard illumination (irradiance 100 mW/cm^2, temperature 25 °C, AM = 1.5 G),[27] the device shows an open circuit voltage (V_{oc}) of 0.6 V and a short circuit current density (J_{sc}) of 5.63 mA/cm^2 (red curve, Figure 3a), corresponding to a power conversion efficiency (η) of 1.6% with a fill factor (FF) of 0.474. Spectral response measurements[27] (Figure 3b) show external quantum efficiencies (EQE) approaching 40% in the device. Integration of the obtained external quantum efficiency data with the true AM1.5G solar emission spectrum matches well with the short-circuit currents obtained under simulated AM1.5G illumination (Figure 3a).

Analysis of these results highlights some important points. First, V_{oc} for our Cu_2S-CdS nanocrystal-based solar cell is better than the best values, 0.54 V,[12] reported for the conventional Cu_2S-CdS thin film solar cells that were widely studied between the 1960s and the 1980s.[12–17] This may be due to the planar junction between Cu_2S and CdS generated during sequential spin coating (total roughness ~4 nm), avoiding the textured junction generated in the "wet" (dipping CdS into CuCl aqueous solution) or "dry" process (formation of Cu_2S by evaporating CuCl on CdS followed by annealing).[16] Furthermore, the performance of the devices is reproducibly achieved without large energy input for high temperature annealing or sintering, which gives our devices a distinct advantage over previous all-inorganic nanocrystal photovoltaic devices.[4]

Two unusual features which were well-studied in the thin film CdS-Cu_2S solar cells are also observed in the system we have prepared. First, the $I-V$ curves measured in the light and dark intersect (Figure 3a). Such behavior was also observed in annealed CdS-Cu_2S thin film cells and labeled as the cross-over effect.[14,16,17] The second unusual effect is that the action spectrum for the solar cells shows a threshold energy that is greater than the band gap of the Cu_2S. There is no photocurrent generated for photons to the red of 700 nm, even though the Cu_2S continues to absorb as far red as 800 nm, and the band offsets of the native components are such that all photogenerated electrons should flow readily to the CdS, and holes to the Cu_2S.

Both effects can be traced to the development of an energetic barrier for electrons in an interfacial zone between the Cu_2S and the CdS layers.[14,15] This spike or barrier in the electron potential arises when Cu ions diffuse a short way into the CdS layer. Photogenerated electrons must have enough energy to overcome this barrier. Further, the cross-over effect in the $I-V$ curve arises again because photoexcited electrons with sufficient energy can overcome this barrier.

The photovoltaic parameters have also been determined as a function of illumination intensity (I). The experimental data (black dots, Figure 3c) show a near-linear relationship (red curve, Figure 3c) between the light intensity and the

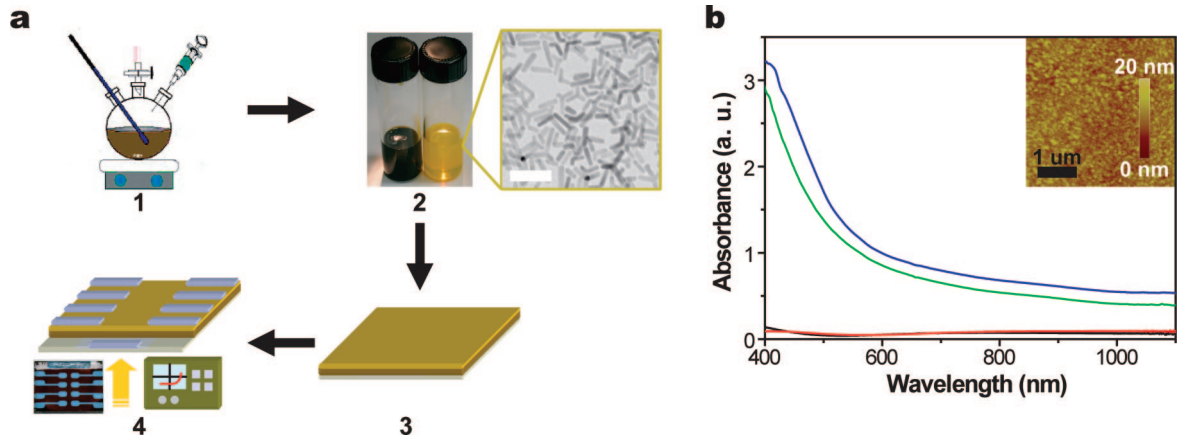

Figure 2. Fabrication and characterization of Cu_2S-CdS nanocrystals photovoltaic devices. (a) Scheme of Cu_2S-CdS nanocrystals photovoltaic device fabrication. (1) Solution-phase synthesizes of Cu_2S nanocrystals and CdS nanorods. (2) Cu_2S nanocrystals and CdS nanorods are cleaned to make stock solutions for photovoltaic device fabrication. Inset, TEM image of CdS nanorods. The scale bar is 50 nm. (3) PEDOT:PSS, Cu_2S nanocrystals, and CdS nanorods are sequentially spin-cast onto ITO-coated glass substrates. (4) Al electrodes are thermally evaporated onto the substrates under high vacuum and electrical measurements are performed. Inset, photography of the Cu_2S-CdS nanocrystals photovoltaic device. (b) UV−vis spectra of ITO-coated glass substrate (black curve), ITO substrate with PEDOT:PSS layer (red curve), ITO substrate with PEDOT:PSS and Cu_2S layers (green curve), and final device (ITO substrate with PEDOT:PSS, Cu_2S, and CdS layers, blue curve). Inset, AFM image of the final device shows an overall roughness less than 4 nm.

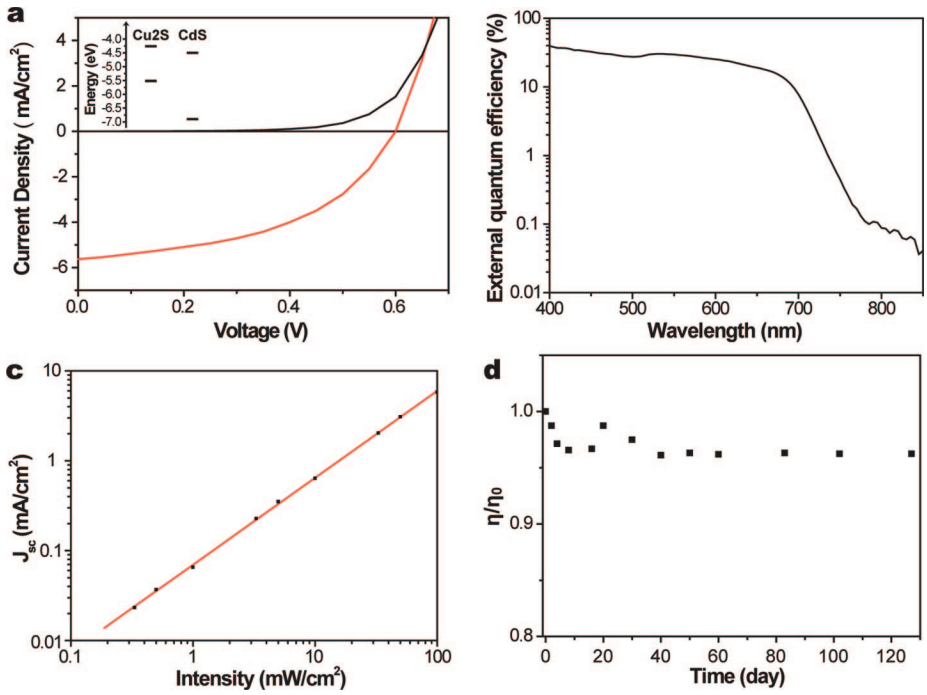

Figure 3. Electrical measurements of Cu_2S-CdS nanocrystals photovoltaic devices. (a) Current density−voltage characteristics of the photovoltaic device under zero illumination (black curve) and standard illumination (red curve, irradiance 100 mW/cm^2, temperature 25 °C, AM = 1.5 G) showing a power conversion efficiency of 1.600%. Inset, band alignment of Cu_2S-CdS. (b) Spectral response measurement showing the external quantum efficiencies approaching 40%. (c) Short circuit current density J_{sc} vs illumination intensity I (black dots) shows a near-linear relationship to a (red curve, $J_{sc} \propto I^n$, with $n = 0.97$). (d) Life time measurement over 120 days shows no significant degradation in efficiency.

short circuit current density: $J_{sc} \propto I^n$, with $n = 0.97$. The near-linear relationship implies only minor charge-carrier recombination is occurring in these photovoltaic devices.[28] Furthermore, during a 4 months measurement period, an encapsulated device shows a nearly constant performance (Figure 3d). This is in contrast to other thin film studies which typically showed degradation in shorter time intervals, due to facile Cu diffusion. It may be that, in our devices, there is a network of necked nanocrystals, and the diffusion of copper through this network is retarded compared with the diffusion in conventional thin films. There is some evidence that a fraction of the dodecanethiol capping ligands survive the film deposition steps (unpublished result), potentially passivating some trap sites and also serving as barrier layers to retard ion diffusion.[29]

Lastly, the ability to fabricate functional nanocrystal solar cells through a simple low temperature solution process suggests the possibility of transferring this technique onto

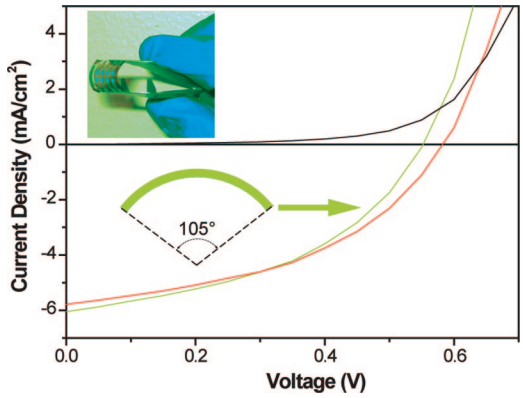

Figure 4. Cu_2S-CdS nanocrystals photovoltaic devices on plastic substrate. Current density−voltage characteristics of the photovoltaic device under zero illumination (black curve) and standard illumination when flat (red curve, 1.604% power conversion efficiency) and released to flat after bent to a curvature of 105° (green curve, 1.472% power conversion efficiency). The decrease in efficiency due to the bending is small (∼8%) given the large stress on the device during the bending and clearly shows the robust nature of our nanocrystal/plastic solar cells. Inset, photograph of the Cu_2S-CdS nanocrystals plastic solar cell.

plastic substrates, which could offer many attractive properties including flexibility, lightweight, shock resistance, softness, and transparency.[30–32] As a demonstration, we fabricated Cu_2S-CdS solar cells on an ITO-coated plastic substrate[26] (upper inset, Figure 4). The device shows a similar performance to the ones fabricated on the conventional ITO glass substrate (red curve, Figure 4. $V_{oc} = 0.574$ V, $J_{sc} = 5.625$ mA/cm^2, FF = 0.494, $\eta = 1.604\%$). In addition, we have investigated the behavior of the nanocrystal solar cell device on the plastic substrate after bending. A comparison of performance recorded when the device was originally flat (red curve, Figure 4) versus released to flat after bent to a curvature of 105° (green curve, Figure 4) shows that there is only a small change after the bending. There is a slight decrease in open circuit voltage ($V_{oc} = 0.552$ V) and a slight increase in short circuit current ($J_{sc} = 6.050$ mA/cm^2) for the device after the bending, corresponding to an overall decrease of power efficiency to 1.472%. This change is small (∼8%) given the large stress on the device during the bending and clearly shows the robust nature of our nanocrystal/plastic solar cells and the potential as the power source for flexible hand-held consumer electronics.

In summary, our studies show that narrow size distribution single crystal Cu_2S nanocrystals can be synthesized in a solution-phase reaction. The incorporation of the Cu_2S nanocrystals into photovoltaic devices yields a power conversion efficiency exceeding 1.6%. Furthermore, the low temperature solution-phase process used to fabricate these nanocrystal solar cell devices opens up the possibility of a promising technique for low-cost power conversion on plastic substrates for future flexible electronics. While the CdS in our device does pose toxicological concerns, Cu_2S, in principle, can be paired with other earth abundant and nontoxic semiconductors to form new sets of photovoltaic materials, which makes the present work a necessary and important intermediate step toward the discovery of these potential systems.

Acknowledgment. We thank Steven Hughes, Jungwon Park, Ching Ting, Jonathan S. Owen, and Paul-Emile Trudeau for helpful discussions. Y.W. thanks the Miller Institute for Basic Research in Science for Miller Research Fellowship. C.W. thanks the Environmental Protection Agency for the EPA STAR Fellowship. This work was supported by DAF AFOSR under Award No. FA9550-06-1-0488 and the Director, Office of Science, Office of Basics Energy Sciences, Materials Sciences and Engineering Division, of the U.S. Department of Energy under Contract No. DE-AC02-05CH11231.

References

(1) Law, M.; Greene, L. E.; Johnson, J. C.; Saykally, R.; Yang, P. D. *Nat. Mater.* **2005**, *4*, 455.
(2) Grätzel, M. *J. Photochem. Photobiol. A* **2004**, *164*, 3.
(3) Baxter, J. B.; Aydil, E. S. *Appl. Phys. Lett.* **2005**, *86*, 053114.
(4) Gur, I.; Fromer, N. A.; Geier, M. L.; Alivisatos, A. P. *Science* **2005**, *310*, 462.
(5) Leschkies, K. S.; Divakar, R.; Basu, J.; Enache-Pommer, E.; Boercker, J. E.; Carter, C. B.; Kortshagen, U. R.; Norris, D. J.; Aydil, E. S. *Nano Lett.* **2007**, *7*, 1793.
(6) Tian, B.; Zheng, X.; Kempa, T. J.; Fang, Y.; Yu, N.; Yu, G.; Huang, J.; Lieber, C. M. *Nature* **2007**, *449*, 885.
(7) Huynh, W. U.; Dittmer, J. J.; Alivisatos, A. P. *Science* **2002**, *295*, 2425.
(8) Gur, I.; Fromer, N. A.; Chen, C.; Kanaras, A. G.; Alivisatos, A. P. *Nano Lett.* **2007**, *7*, 409.
(9) Cui, D. H.; Xu, J.; Zhu, T.; Paradee, G.; Ashok, S.; Gerhold, M. *Appl. Phys. Lett.* **2006**, *88*, 183111.
(10) Beek, W. J. E.; Wienk, M. M.; Janssen, R. A. J. *Adv. Mater.* **2004**, *16*, 1009.
(11) Liu, G.; Schulmeyer, T.; Brötz, J.; Klein, A.; Jaegermann, W. *Thin Solid Films* **2003**, *431−432*, 477.
(12) Rothwarf, A.; Barnett, A. M. *IEEE T. Electron Dev.* **1977**, *24*, 381.
(13) Böer, K. W. *J. Cryst. Growth* **1982**, *59*, 111.
(14) Gill, W. D.; Bube, R. H. *J. Appl. Phys.* **1970**, *41*, 3731.
(15) Fahrenbr, A. L.; Bube, R. H. *J. Appl. Phys.* **1974**, *45*, 1264.
(16) Pfisterer, F. *Thin Solid Films* **2003**, *431*, 470.
(17) Rothwarf, A. *Solar Cells* **1980**, *2*, 115.
(18) Yong, K.; Sahoo, Y.; Swihart, M. T.; Prasad, P. N. *J. Phys. Chem. C* **2007**, *111*, 2447.
(19) Li, Y.; Liao, H.; Ding, Y.; Qian, Y.; Yang, L.; Zhou, G. *Chem. Mater.* **1998**, *10*, 2301.
(20) Peng, Z. A.; Peng, X. *J. Am. Chem. Soc.* **2001**, *123*, 183.
(21) Sigman, M. B.; Ghezelbash, A.; Hanrath, T.; Saunders, A. E.; Lee, F.; Korgel, B. A. *J. Am. Chem. Soc.* **2003**, *125*, 16050.
(22) Brelle, M. C.; Torres-Martinez, C. L.; McNulty, J. C.; Mehra, R. K.; Zhang, J. Z. *Pure Appl. Chem.* **2000**, *72*, 101.
(23) Ghezelbash, A.; Korgel, B. A. *Langmuir* **2005**, *21*, 9451.
(24) All chemicals are purchased from Aldrich, and used without any further purification. In a typical synthesis of Cu_2S nanocrystals, 1.25 mmol of ammonium diethyldithiocarbamate is mixed with 10 mL of dodecanethiol and 17 mL of oleic acid in a three-neck flask. The solution is heated up to 110 °C under Argon (Ar) flow followed by a quick injection of a suspension composed of 1 mmol of copper(II) acetylacetonate and 3 mL of oleic acid. Then, the solution is quickly heated up to 180 °C and kept at the temperature for 10−20 min. The cleaning of the nanocrystals involves multiple steps performed in a glovebox with Ar protection, and all of the solvents used are anhydrous to avoid any possible oxidation. Right after the reaction, the solution containing Cu_2S nanocrystals is cooled down naturally to 120 °C before being taken out of the flask for centrifuging at 4600 rpm for 10 min. The supernatant is discarded and the precipitation is first fully dissolved in 4 g of toluene and then precipitated out by adding11g of isopropanol followed by centrifuging at 4600 rpm for 10 min. This procedure is repeated three times to clean away the residue of dodecanethiol and oleic acid. The synthesis of the CdS nanorods is conducted in a similar manner mention above and the exact details can be found in ref 18. After that, the Cu_2S nanocrystals and the CdS nanorods are dissolved

separately into 15 mL pyridine and kept at 120 °C for at least one day, allowing for comprehensive ligand exchange, followed by precipitated out using appropriate amount of hexane. The Cu_2S nanocrystals and the CdS nanorods are then dissolved separately into appropriate amounts of chloroform ($CHCl_3$) and then passed through a 0.4 μm Teflon filter to make stock solutions for photovoltaic device fabrication.

(25) UV−vis absorption spectrum is recorded from Cu_2S nanocrystals dispersed in chloroform at room temperature. Photoluminescence spectrum is obtained from Cu_2S nanocrystals dispersed in tetrachloroethylene at room temperature using both CCD and InGaAs detectors.

(26) Glass substrates coated with 150 nm ITO (Thin Film Devices Inc., resistivity 20 ohms/sq) are cleaned by ultrasonication for ca. 30 min in an even mixture of acetone and isopropanol and then deionized water, respectively. The substrates are then dried under a stream of nitrogen followed by oxygen plasma cleaning for 15 min at 0.2 torr. A filtered dispersion of PEDOT:PSS in water (Baytron-PH) was immediately spin-cast at 4000 rpm for 1 min and then baked for 30 min at 120 °C. After cooling down, nanocrystal films are spin-cast at 600 rpm onto the substrates. To create bilayer structures, Cu_2S films are spin-cast first and then heated for 10 min at 150 °C to remove excess solvent and allow for spin-casting of the second films of CdS. Then, the substrates are annealed again for 5∼10 min at 150 °C. After that, the substrates are held at ca. 10^{-7} torr for up to 12 h, after which 200 nm of top aluminum (Al) electrodes are deposited by thermal evaporation through a shadow mask, resulting in individual devices with 0.04 cm^2 nominal areas. After evaporation, a rapid thermal annealing is performed on the devices at 150 °C for 30∼60 seconds. The procedure of fabricating photovoltaic device on plastic substrate is same as above except ITO-coated plastic substrates (OC50, CP Films) are used to replace the regular ITO-coated glass substrates. Accordingly, the oxygen plasma cleaning time is reduced to 3.5 min.

(27) Simulated AM1.5G illumination is obtained with a Spectra Physics Oriel 300W Solar Simulator with AM1.5G filter set. The integrated intensity is set to 100 mW/cm^2 using a thermopile radiant power meter (Spectra Physics Oriel, model 70260) with fused silica window, and verified with a Hamamatsu S1787−04 diode. Intensity is controlled to be constant throughout measurements with a digital exposure controller (Spectra Physics Oriel, model 68950).

(28) Nelson, J. *Phys. Rev. B* **2003**, *67*, 155209.

(29) Yang, H.; Holloway, P. H. *Appl. Phys. Lett.* **2003**, *82*, 1965.

(30) Mcalpine, M. C.; Friedman, R. S.; Lieber, C. M. *Proc. IEEE* **2005**, *93*, 1357.

(31) McAlpine, M. C.; Ahmad, H.; Wang, D.; Heath, J. R. *Nat. Mater.* **2007**, *6*, 379.

(32) Sun, Y.; Rogers, J. A. *Adv. Mater.* **2007**, *19*, 1897.

NL801817D